



Science Arts & Métiers (SAM)

is an open access repository that collects the work of Arts et Métiers Institute of Technology researchers and makes it freely available over the web where possible.

This is an author-deposited version published in: <https://sam.ensam.eu>
Handle ID: <http://hdl.handle.net/10985/18917>

To cite this version :

Sabeur MSOLLI, Mohamed BEN BETTAIEB, Farid ABED-MERAIM - Modeling of void coalescence initiation and its impact on the prediction of material failure - In: ESAFORM 2016, France, 2016-04-27 - Proceedings of the 19th International ESAFORM Conference on Material Forming - 2016

Any correspondence concerning this service should be sent to the repository

Administrator : scienceouverte@ensam.eu



Modeling of void coalescence initiation and its impact on the prediction of material failure

Sabeur Msolli^{1, a)}, Mohamed Ben Bettaieb^{1, b)} and Farid Abed-Meraim^{1, c)}

¹LEM3, UMR CNRS 7239 – Arts et Métiers ParisTech, 4 rue Augustin Fresnel, 57078 Metz Cedex 3, France
DAMAS, Laboratory of Excellence on Design of Alloy Metals for low-mAss Structures, Université de Lorraine, France

^{a)} Corresponding author: Sabeur.Msolli@ensam.eu

^{b)} Mohamed.Benbettaieb@ensam.eu

^{c)} Farid.Abed-Meraim@ensam.eu

Abstract. In the present paper, Thomason's criterion is coupled with the well-known Gurson–Tvergaard–Needleman (GTN) damage model and used for the determination of the critical void volume fraction f_c , which marks the initiation of the coalescence stage. The onset of void coalescence predicted by Thomason's criterion is compared to that obtained by using a predefined f_c , which is usually fitted on the basis of experimental results, as originally proposed in the GTN model. Comparisons are made in terms of both single finite element simulations and numerical results of deep drawing of a cup.

INTRODUCTION

The prediction of the formability of sheet metal parts is a quite important task nowadays. Under severe forming operations, drawn parts are often exposed to failure due to crack initiation and propagation. Among the key mechanisms that are likely to promote the occurrence of cracks, one can quote the nucleation, growth and coalescence of voids in the sheet material. The degradation is also compounded by the presence of initial defects or initial void volume fraction. At the coalescence stage, a drop in the material stiffness is recorded and failure proceeds. In order to describe the material behavior, dependent on the evolution of void volume fraction, several models have been developed in the literature. Gurson–Tvergaard–Needleman (GTN) model may be considered as one of the most popular damage models [7]. It has been applied for the modeling of material damage behavior from nucleation to coalescence and proved its efficiency in many applications. This model has also been extended to account for kinematic hardening [2] and has been used to predict the ductility limit of thin metal sheets [4]. However, issues relating to the critical void volume fraction f_c still rely on experimental measures. The resulting value of f_c , as measured experimentally, often depends on the initial void volume fraction f_0 . Also, the variation of f_c with the stress triaxiality has been investigated by many authors (see, for instance, [5]). It appears that considering f_c as constant, for a given material under variable loading and/or different values of f_0 , is a strong assumption. Thanks to Thomason's limit load criterion, a value for f_c can be numerically determined, which ensures a continuous and physically-based transition between the stages of growth and coalescence [12]. This criterion is based on the loss of stability of the plastic flow. The onset of coalescence is activated when Thomason's criterion is verified. At this level, f_c is fixed to the value of the void volume fraction f . It will be shown in this

paper that the value of f_c determined from Thomason's criterion may be quite different from its counterpart experimentally fitted. These differences will be shown either for monotonic or non-monotonic loading paths, as it is the case in deep drawing. These findings are important due to their implications on ductile failure predictions of sheet metals during deep drawing in terms of the critical strain at failure as well as the specific location of the failure zone.

GURSON-TVERGAARD-NEEDLEMAN DAMAGE MODEL

The constitutive framework of the GTN damage model is described by the following main equations:

- The expression of the GTN yield function:

$$\Phi_{GTN} = \left(\frac{q}{\bar{\sigma}} \right)^2 + 2q_1 f^* \cosh \left(-\frac{3q_2 p}{2\bar{\sigma}} \right) - 1 - q_3 f^{*2}, \quad (1)$$

where $q = \sqrt{3\boldsymbol{\Sigma}_d : \boldsymbol{\Sigma}_d} / 2$ and $p = -tr(\boldsymbol{\Sigma}) / 3$ are, respectively, the equivalent macroscopic stress and the hydrostatic pressure associated with the macroscopic stress tensor $\boldsymbol{\Sigma}$, $\bar{\sigma}$ is the flow stress of the fully dense matrix, f^* is the modified volume fraction of voids and q_1 , q_2 and q_3 are material constants. f^* is introduced in order to improve the description of the coalescence stage. In this case, one can express f^* by using the following empirical equation:

$$f^* = f_c + \delta_{GTN} (f - f_c) \quad \text{where} \quad \delta_{GTN} = \begin{cases} 1 & \text{if } f \leq f_c \\ \frac{f_u - f_c}{f_F - f_c} & \text{if } f_c < f < f_F \end{cases}. \quad (2)$$

In the previous equation, f_F represents the final volume fraction prior to failure, while f_u is mainly expressed as function of the parameters q_1 , q_2 and q_3 :

$$f_u = (q_1 + \sqrt{q_1^2 - q_3}) / q_3. \quad (3)$$

- The evolution of the void volume fraction:

The evolution of the void volume fraction is modeled such that the porosity rate \dot{f} is additively decomposed into nucleation and growth parts, denoted \dot{f}_n and \dot{f}_g , respectively

$$\dot{f} = \dot{f}_n + \dot{f}_g = \frac{f_N}{s_N \sqrt{2\pi}} \exp \left[-\frac{1}{2} \left(\frac{\bar{\varepsilon}^p - \varepsilon_N}{s_N} \right)^2 \right] \dot{\bar{\varepsilon}}^p + (1 - f) tr(\mathbf{D}^p), \quad (4)$$

where \mathbf{D}^p is the macroscopic plastic strain rate tensor related to Φ_{GTN} by the normality rule $\mathbf{D}^p = \dot{\gamma} (\partial \Phi_{GTN} / \partial \boldsymbol{\Sigma})$, in which $\dot{\gamma}$ denotes the plastic multiplier. f_N represents the volume fraction of inclusions that are likely to nucleate, ε_N refers to the equivalent plastic strain for which half of the inclusions have nucleated, and s_N is the standard deviation on ε_N .

- The expression of the flow stress $\bar{\sigma}$ of the fully dense matrix, which is defined by the Swift law:

$$\bar{\sigma} = K (\varepsilon_0 + \bar{\varepsilon}^p)^n, \quad (5)$$

where $\bar{\varepsilon}^p$ is the equivalent plastic strain of the fully dense matrix, and K , n and ε_0 are hardening parameters.

- The equivalence between the rates of macroscopic and matrix plastic work:

$$(1-f)\bar{\sigma} \dot{\bar{\epsilon}}^p = \boldsymbol{\Sigma} : \mathbf{D}^p. \quad (6)$$

THOMASON COALESCENCE CRITERION

Thomason's criterion is based on the fact that void coalescence is enabled when the plastic limit load condition is reached for localized deformation of intervold matrix ([10], [11], [12]). In this paper, voids are assumed to be initially spherical and remain spherical during the deformation. Thomason's criterion states that no coalescence occurs so long as the following condition is satisfied ([14], [15]):

$$\frac{\Sigma_{\max}}{\bar{\sigma}} < (1-\pi\chi^2) \mathcal{C}_f = F(\chi) \quad \text{with} \quad \mathcal{C}_f = \left(\alpha(n) \left(\frac{1-\chi}{\chi} \right)^2 + \frac{\beta}{\sqrt{\chi}} \right). \quad (7)$$

In the previous equation, Σ_{\max} refers to the maximal principal value of $\boldsymbol{\Sigma}$, while $\alpha(n)$ and $\beta(n)$ are parameters that may depend on the hardening exponent n , which ranges between 0 and 0.3. Pardoen and Hutchinson propose in ([8], [9]) the following expression for $\alpha(n)$:

$$\alpha(n) = 0.1 + 0.217n + 4.83n^2. \quad (8)$$

However, parameter β is set to 1.24, as suggested by Pardoen and Hutchinson ([8], [9]).

As to χ , which appears in Eq. (7), it refers to the void space ratio, defined as the ratio of the void diameter to the void spacing. The expression of this ratio is given by

$$\chi = \frac{\left(\frac{6f}{\pi} \exp(\varepsilon_1 + \varepsilon_2 + \varepsilon_3) \right)^{1/3}}{\sqrt{\exp(\varepsilon_1 + \varepsilon_2 + \varepsilon_3 - \varepsilon_{\max})}}, \quad (9)$$

where ε_1 , ε_2 and ε_3 are the principal macroscopic strains, while ε_{\max} is equal to $\text{Max}(\varepsilon_1, \varepsilon_2, \varepsilon_3)$.

NUMERICAL RESULTS

The constitutive equations presented previously are numerically integrated by using an implicit time integration scheme, as described by Aravas [1], and implemented as a user material (UMAT) subroutine in Abaqus/Standard®. Thomason's criterion is used to determine the value of f_c . First, the accuracy of the implemented algorithm is evaluated through numerical simulation on a single finite element. Some results from the literature using Thomason's criterion are taken for validation purposes. Then, the simulation results for a uniaxial tensile test obtained by using Thomason's criterion are compared with those associated with a predefined value for f_c (fitted on the basis of experimental observations). It will be emphasized that, for a given material, the critical void volume fraction obtained from Thomason's criterion may be significantly different from the predefined f_c . Finally, finite element modeling of a deep drawing test is performed to show the impact, on the material response, of a predefined value of f_c as compared to that computed using Thomason's criterion.

Single finite element simulation

The aim of this section is twofold: (i) to validate the numerical implementation by comparing the corresponding results with those obtained from the literature, and (ii) to compare the results given by a predefined and a computed value of f_c , respectively. The material parameters for a 4340 steel material identified in [13] are used in this

simulation. In the latter framework, the Johnson–Cook hardening model has been adopted for the matrix material [13]. The material parameters of the Swift model are fitted on the basis of the stress–strain curve obtained by the Johnson–Cook hardening model. For the numerical simulation, a single C3D8 finite element is considered for the simulation of the uniaxial tensile test. The loading and boundary conditions are presented in FIGURE 1.

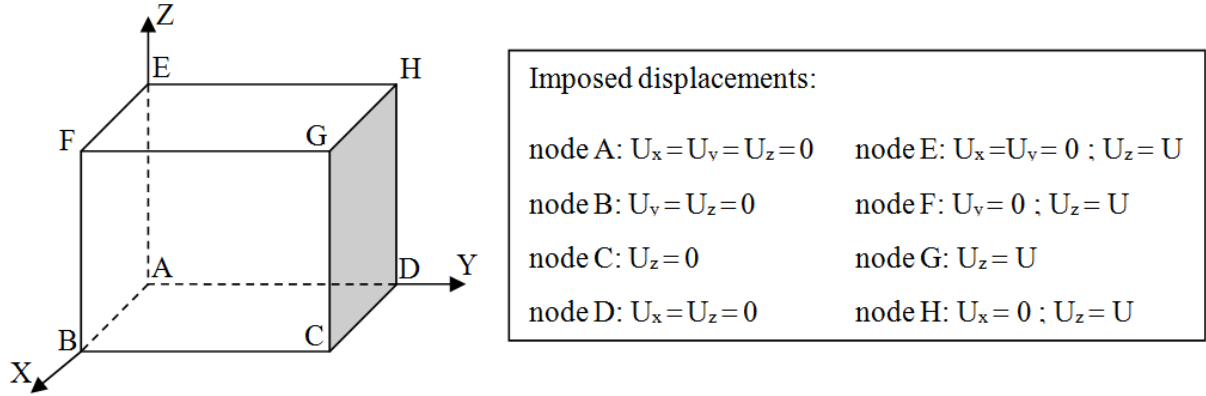
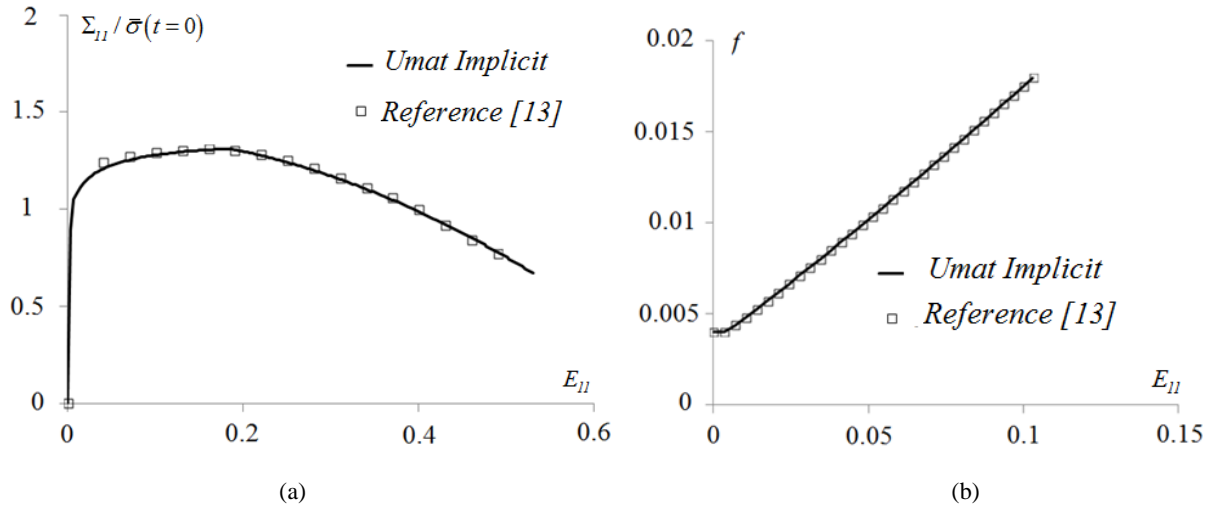
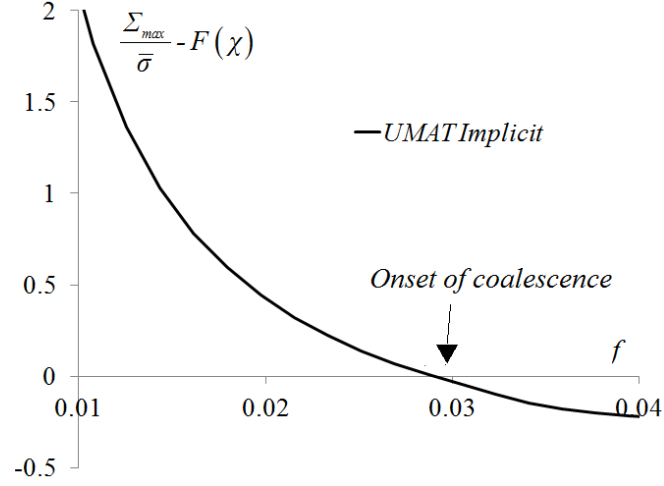


FIGURE 1. Loading and boundary conditions applied to a single finite element.

Our predictions are compared in FIGURE 2 with the results available in [13]. The results are almost indistinguishable. Thomason’s criterion permits to predict the onset of coalescence at $f_c = 0.03$ (see FIGURE 2(c)). FIGURE 2 suggests that some degree of confidence could be accorded to the implemented model, which is able to reproduce the tensile behavior of the 4340 steel material considered.





(c)

FIGURE 2. Predictions of the GTN model coupled with Thomason's criterion for a uniaxial tensile test, with comparison to [13].

(a) Stress–strain curves; (b) Evolution of the void volume fraction; (c) Evolution of Thomason's factor $\frac{\Sigma_{max}}{\bar{\sigma}} - F(\chi)$.

A second simulation is performed on an Al5182 material, whose associated model parameters are available in ([3], [6]), and summarized in TABLE 1. The value of the predefined f_c is calibrated by using experimental results and is also given in TABLE 1. In the subsequent simulation, comparisons of uniaxial tensile responses are made to reveal the effect of coalescence initiation modeling (i.e., predefined versus criterion-computed values for f_c). The results of the uniaxial tensile test simulation presented in FIGURE 3 show clear differences between the responses. Whereas f_c is predefined as “constant”, equal to 0.00213 in the first simulation, a value of f_c of 0.027 is found when using Thomason's criterion. It is well known that Thomason's criterion takes into account the relationship between χ and f . The evolution of χ leads to the translation of the constraint factor \mathcal{C}_f involved in the criterion, until the onset of coalescence is predicted ([14]).

TABLE 1. Material parameters for the Al5182 material

$E [MPa]$	ν	n	$K [MPa]$	ε_0	f_0	f_c	δ_{GTN}	q_1	q_2	q_3	s_N	ε_N	f_N
70000	0.33	0.17	371.2	0.00324	10^{-3}	0.00213	10	1	1.5	2.15	0.1	0.27	0.035

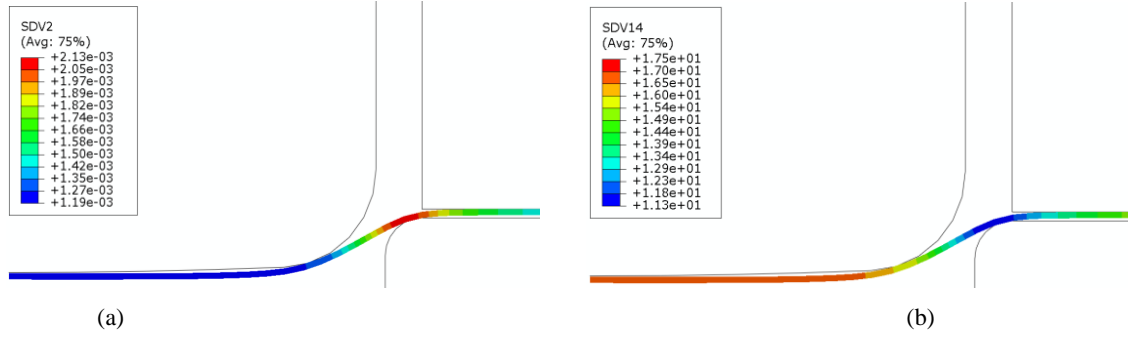


FIGURE 5. Results of the simulation using the GTN model with Thomason's criterion. (a) f has already reached the predefined value of f_c . (b) Thomason's criterion is not yet reached at this level.

CONCLUSION

The GTN model with the embedded Thomason criterion has been numerically integrated and implemented in the finite element code Abaqus. The results of the simulations using a single finite element were compared with some available data and show good repeatability. Other simulations reveal that the value of f_c computed by using Thomason's criterion could be quite different from the predefined value of f_c , as being fitted from experimental stress-strain curves. The predicted value of f_c is often higher, which implies a delay in the onset of coalescence. In the same way, the simulation of the deep drawing of a cup indicates that, when f reaches the predefined value of f_c , the Thomason criterion is not satisfied yet. These observations confirm the need for precise modeling of the coalescence initiation, as this has significant implications in the prediction of failure during complex material processes, such as sheet metal forming.

REFERENCES

1. N. Aravas. Int J NumMeth Eng **24**, 1395–1416 (1987).
2. M. Ben Bettaieb, X. Lemoine, L. Duchêne, and A.-M. Habraken. Int J Num Meth Eng **85**, 1049–1072 (2011).
3. M. Brunet, S. Mguil, and F. Morestin, J Mater Process Tech **80–81**, 40–46 (1998).
4. H. Chalal and F. Abed-Meraim, Mech Mater **91**, 52–166 (2015).
5. J. Koplik and A. Needleman. Int J Solids Struct **24**, 835–853 (1988).
6. L.Z. Mansouri, H. Chalal, and F. Abed-Meraim, Mech Mater **76**, 64–92 (2014).
7. A. Needleman and V. Tvergaard. Eng Fract Mech **38**, 157–173 (1991).
8. T. Pardoen and J.W. Hutchinson, J Mech Phys Solids **48**, 2467–2512 (2000).
9. T. Pardoen, Y. Marchal, and F. Delannay, Eng Fract Mech **69**, 617–631 (2002).
10. P.F. Thomason, Acta Metall Mater **33**, 1087–1095 (1985).
11. P.F. Thomason, Acta Metall Mater **40**, 241–249 (1992).
12. P.F. Thomason, Acta Metall Mater **41**, 2127–2134 (1993).
13. G. Vadillo, R. Zaera, and J. Fernández-Sáñez, Comput Method Appl M **197**, 1280–1295 (2008).
14. Z.L. Zhang and E. Niemi, Eng Fract Mech **48**, 529–540 (1994).
15. Z.L. Zhang, C. Thaulow, and J. Odegard, Eng Fract Mech **67**, 155–168 (2000).